The Stress Triggering Role of the 1923 Kanto Earthquake.

M. Nyst,[1,2] N. Hamada,[3] F. F. Pollitz,[1] and W. Thatcher[1]

M. Nyst, Department of Geophysics, Stanford University, Stanford, USA. (mnyst@pangea.stanford.edu)

[1]U. S. Geological Survey, Menlo Park, USA

[2]Now at Department of Geophysics, Stanford University, Stanford, USA

[3]Seismology and Volcanology Research Department, Meteorological Research Institute Japan, Meteorological Agency, Tsukuba, Japan

Abstract. This study uses a new source model for the 1923 M_s=7.9 Kanto earthquake in Japan, proposed in an accompanying paper, to compute its influence on the static stress field in the Kanto region. Coseismic stress changes calculated with the two-plane, uniform source model and performed under Coulomb failure assumptions show a general spatial consistency with the regional seismicity rate changes associated with the 1923 earthquake. Positive changes in Coulomb failure stress in Odawara and central Boso coincide with clusters of aftershocks and a drop in Coulomb failure stress around Tokyo agrees with the still ongoing seismic quiescence. We also compute the coseismic Coulomb stress change on different sources of seismic hazard in the Kanto region and find that active faults in the Tokyo Bay area were affected by the 1923 earthquake. The Coulomb stress level increased on Izu Peninsula, which may have triggered the 1930 $M_s = 7.3$ Kita-Izu earthquake. Furthermore, Coulomb stress increase on the Western Sagami Bay fracture is inconsistent with this structure's presumed delayed rupture. Finally, Coulomb stresses were also raised on the down-dip extension of the 1923 rupture plane, and on the 1703 earthquake fault plane southeast of Boso Peninsula, bringing these structures closer to failure.

1. Introduction

The highly destructive 1923 $M_s = 7.9$ Kanto earthquake in Japan caused the deaths of over 140,000 people and destroyed Yokohama and large parts of Tokyo. At present the Tokyo Bay region houses more than 30 million people. It dominates Japan's economy, politics, trade, finance, arts and communication. A similar earthquake today would not only cause a human tragedy of enormous proportions, but would also have catastrophic effects on the Japanese and world economies. For assessment of the current seismic hazard in the Tokyo Bay region it is crucial to establish the influence of the Kanto earthquake on the regional stress field. In an accompanying paper *Nyst et al.* [2005] derive a new source model that optimally fits a newly augmented set of historic geodetic measurements of the coseismic deformation. In this paper we use this model to calculate changes in the static stress field caused by the earthquake that may have influenced subsequent seismicity.

The earthquake nucleated in the Odawara region and ruptured the plate interface in the Sagami trough [Kanamori and Miyamura, 1970; *Ando,* 1971; *Kanamori,* 1971] (Figure 1B). Here the Philippine Sea plate subducts in northwestward direction at an highly oblique angle to the boundary with the overriding northern Honshu block [e.g., *Seno et al.,* 1993; *Heki et al.,* 1999] (Figure 1A). Arc-arc collision north of Izu Peninsula determines the surface deformation west of the Sagami trough [e.g., *Huchon and Kitazato,* 1984; Sagiya et al., 2000]. The westward directed convergence of the Pacific plate with respect to northern Honshu is accommodated by subduction of the Pacific plate along the Japan trench.

Okada [2001] showed that the patterns of seismicity distribution in the Kanto region before and after the 1923 earthquake are significantly different. He also concluded that the 1923 earthquake is probably still influencing the present-day seismicity. In another recent study *Hamada et al.* [2001] give a detailed account of the aftershock activity of the 1923 earthquake in the first 4 months after the earthquake. Here we test whether changes in the three-dimensional Coulomb failure stress field due to the 1923 Kanto earthquake can explain the changes in the seismicity distribution after 1923, as observed by *Okada* [2001], as well as the distribution of aftershocks from the 1923 catalogue of *Hamada et al.* [2001]. First we present results that show relatively good correlation between Coulomb failure stress change and seismicity rate changes in the Kanto region. Then we examine Coulomb stress changes on active faults and other sources of seismic hazard in the Kanto region to determine their relative change in failure potential.

2. Seismicity observations

Okada [2001] presents a compilation of all earthquakes with magnitude > 6 and depths not exceeding 60 km that occurred in Kanto between 1884 and 2001 (Figure 2A,B, and C). The earthquake catalogue by *Hamada et al.* [2001] contains the locations, magnitudes and timing of all earthquakes recorded during the first 4 months immediately after the Kanto earthquake (Figure 2D). The compilation of *Okada* [2001] includes *Hamada et al.'s* [2001] $M > 6$ Kanto earthquake aftershocks (light-blue in Figure 2B).

Some characteristics of the spatial distribution of the aftershock activity agrees reasonably well with the pattern of postseismic change in the larger-scale seismicity. A dense cluster of aftershocks occurred in the western part of Kanagawa Prefecture between the Earth's surface and 40 km depth (red dashed circle number 1 in Figure 2D). *Okada* [2001]

detects an increase in the occurrence of larger-scale earthquakes in this same region during the first 10 years after the earthquake with respect to the 40 years preceding the earthquake (Figure 2A and B). Furthermore, after the 1923 Kanto earthquake an area covering the Tokyo Bay and Miura Peninsula experienced a seismicity rate decrease with respect to the 40 years before the earthquake. This seismic quiescence is still ongoing today (Figure 2A, B and C). The region around Tokyo is characterized by an absence of aftershocks between 0 and 40 km depth (red dashed ellipse number 3 in Figure 2D).

A cluster of aftershocks hit central Boso (red dashed ellipse in Figure 2D) between the Earth's surface and about 40 km depth. In this area, *Hamada et al.'s* [2001] aftershock catalogue differs from *Okada's* [2001] seismic compilation, in which during the first 10 postseismic years central Boso remained clear from $M > 6$ earthquakes. A possible explanation for this discrepancy is the poor determination of the positions of the 4 $M > 6$ 1923 aftershocks south of Boso Peninsula. These aftershocks represent an area of postseismic rate increase in *Okada's* [2001] compilation (Figure 2B). Their positions are determined by *Hamada et al.* [2001], who state that the uncertainty in the position of the off-shore aftershocks in the Sagami Bay is larger than 20 km. If we assume an uncertainty of 40 km in their position estimates, these $M > 6$ Sagami Bay aftershocks could be located on Boso Peninsula. At present, little seismic activity is detected on Boso Peninsula (Figure 2C). From studying the Japan Meteorological Agency (JMA) catalogue *Hamada et al.* [2001] concludes that the seismicity rate increase on Boso Peninsula lasted for only a few years until 1926.

3. Earthquake source model

In this study we use the earthquake source model based on geodetic observations by *Nyst et al.* [2005]. We refer to *Nyst et al.* [2005] for a detailed description of model derivation and characteristics, other geodetic models and the data set. Here we only briefly summarize the main properties of the model.

The source model describes the earthquake as dislocations on two adjacent ≈20° dipping low-angle fault planes in the Sagami Trough. The planes are rectangular with horizontal upper and lower boundaries in a isotropic, elastic uniform half-space [*Okada,* 1985, 1992]. The planes accommodate reverse dextral slip of 9.5 m and 6.0 m with azimuths of 121° and 163°, respectively (Figure 3). Like previous models based on geodetic data [*Ando,* 1971, 1974; *Matsu'ura et al.,* 1980; *Matsu'ura and Iwasaki,* 1983; *Wald and Somerville,* 1995; *Pollitz et al.,* 1995; *Kabayashi and Koketsu; Sato et al.,* 2005] it is based on observations from leveling and first order triangulation measurements that were obtained in campaigns between 1883 and 1927. Unique aspects of the data set of *Nyst et al.* [2005] are the use of angle changes rather than displacements, to avoid some major sources of systematic error, the application of a correction to remove interseismic deformation based on continuous GPS between 1998 and 2001 [*Nishimura and Sagiya,* 2004] and the inclusion of a large number of second order triangulation data that densely sample the Kanto plain. Compared to earlier models the final uniform-slip model of *Nyst et al.* [2005] fits the data set best in a normalized root-mean square sense.

4. Modeling coseismic stress transfer

The change in Coulomb failure stress (ΔCFS):

$$\Delta CFS = \Delta|\vec{\tau}| + \mu(\Delta\sigma + \Delta p) \tag{1}$$

depends on μ the coefficient of friction, assumed to be constant over time, τ magnitude of the shear traction on a plane, σ normal traction (positive for tension) on the plane and p the pore fluid pressure, while assuming that the cohesion of the fault surface remains constant over time [e.g., *Jaeger and Cook*, 1969; *Harris*, 1998]. We compute ΔCFS with our preferred two-plane unform fault model (Section 3) using Coulomb failure assumptions. Under Coulomb failure assumptions faults are advanced towards failure, if they are located in regions where the earthquake-induced stress is increased in the preferred orientation of fault slip [*Stein et al.*, 1997]. In our analysis we look for correlation between the spatial pattern of ΔCFS and the spatial pattern of aftershocks.

It is important to note here that we only have a detailed account of the seismicity in the first 4 months after the earthquake, by means of the aftershock catalogue of *Hamada et al.* [2001]. The changes in seismicity rate as observed by *Okada* [2001] are in terms of large magnitude earthquakes (M>6 instead of M>3) over relatively long periods of time (years instead of months). Consequently, a comparison between preseismic and postseismic activity in Kanto is uncertain. Our inferences of seismicity rate changes induced by the 1923 earthquake in the different identified areas are based on the assumption that the distribution of larger-magnitude earthquakes represents the seismicity rate on all magnitude scales. Even though there is a reasonably good correlation between the distribution of aftershocks and present-day seismicity, this assumption is not necessarily straightforward. This is illustrated by the dense cluster of aftershocks on Boso Peninsula, whereas *Okada's* [2001] study does not detect any significant larger-magnitude seismic activity in the first few years after the 1923 earthquake. Nonetheless, we adopt the assumption of self-consistency in our analysis of the stress field, because no more information is available.

The focal mechanisms of the aftershocks in *Hamada et al.'s* [2001] catalogue are unknown. To determine regionally preferred orientations of failure we use information from focal mechanisms of shallow earthquakes (M>2, depth $\leq$ 40 km) from the JMA catalogue that covers the time period from 1997 to 2003. The resulting average focal mechanisms found per region for which we identified postseismic changes in the seismicity pattern are shown in Figure 4A. The stress orientations in the areas of Kanagawa Prefecture and Boso Peninsula between 0 and 30 km depth and around Tokyo between 0 and 40 km depth reflect the relative plate motion direction: These regions are mainly dominated by small magnitude thrust events with NNW-SSE directed contraction. We find that the general features of the derived preferred orientations of failure per region are consistent with focal mechanisms of large-scale earthquakes (magnitude > 5) of the Harvard Centroid Moment Tensor (HCMT) and JMA catalogs (Figure 4A) and with directions of the maximum horizontal stress component from borehole data (Figure 4B) [*Tsukahara and Ikeda*, 1987], where these data types were obtained. As the regional preferred orientation of failure we adopt contraction (at a rake of 90°) with a NNW-SSE orientation (at a strike of 250°).

5. Results

5.1. Comparison between ΔCFS and seismic activity in Kanto

Figure 5 shows the Coulomb stress changes on area-specific thrust faults in the Tokyo bay area for different depths. We find good correlation between aftershock localization and increased stress levels at depths of about 15 to 20 km. In Kanagawa Prefecture from the aftershocks that occur outside the immediate source area of the 1923 earthquake and in the area of increased seismicity at a depth of about 15 km (Figure 5A) a percentage of 94% is located within the zone that is characterized by a positive ΔCFS_m. The decrease

in Coulomb failure stress at a depth of 20 km for the small area around Tokyo agrees with the observed decrease in seismic activity (Figure 2A and B) and the almost complete absence of aftershock activity (Figure 5B). 84% of the aftershocks in the dense cluster observed between 1923 and 1926 on Boso Peninsula at a depth of about 15 km (Figure 5A) coincides with an area of positive ΔCFS_t, computed in a pure thrusting regime.

6. Discussion: Sources for seismic hazard in Kanto

In the previous section we show that the main features of the seismicity rate changes in the Kanto area after the 1923 Kanto earthquake can be explained by changes in the Coulomb failure stress induced by the earthquake. Adopting Coulomb failure stress assumptions we investigate how the 1923 earthquake has changed the stress field on the main sources of seismic hazard in the Kanto region [e.g., *Okada*, 2001]. Since we do not incorporate the regional seismic history and its associated stress evolution these values are only relative to the state of stress before the earthquake.

6.1. Honshu intraplate earthquake

A strong Honshu intraplate event has not yet unequivocally been observed. Based on a study of wave propagation in a three-dimensional Earth model, *Furumura* [2003] proposes the 1855 $M_s = 7.2$ Ansei Edo earthquake as a possible candidate. The epicenter of the 1855 Ansei Edo earthquake is indicated in Figure 5A. If this earthquake was located on a shallow fault, this fault underwent a stress drop due to the Kanto earthquake according to our Coulomb calculations for this area (Figure 5A).

6.2. Interplate event between Philippine Sea and northern Honshu plates

The upper 30 km of the Philippine Sea - northern Honshu plate interface has generated the most damaging earthquakes in Tokyo's history [e.g., *Matsuda,* 1978]. The last big event before 1923 was the 1703 Genroku M_s=8.1 earthquake with its epicenter located southeast of the 1923 epicenter. This event is thought to have ruptured the entire 1923 fault plane in addition to a part of the interface situated immediately east of the 1923 Kanto fault plane [*Matsuda,* 1978; *Shishikura,* 2003]. *Matsuda* [1978] locates this eastern plane along the Sagami trough in the eastward extension of the 1923 plane. The 1923 earthquake increased the Coulomb failure stress regime on this fault plane (Figure 7A). *Shishikura* [2003] argues that the distinct pattern of vertical displacements of the 1703 Genroku terraces along the eastern shoreline of Boso Peninsula, with a maximum of up to 5 m in southern Boso, requires 12 m of slip on a smaller fault plane that strikes in NE direction, i.e. at a 45° angle with the 1923 fault plane (Figure 7B). He finds 6.7 m of slip on the western (Kanto) fault plane for the 1703 event, which is of the order of our results of 6 m for slip on this fault plane for the 1923 event. The geological marine terrace records over the last 7500 years show that a Genroku-type event occurs every 2000 to 2700 years. Assuming that all relative plate motion is released by earthquakes, coseismic slip of 12 m with a recurrence interval of 2000 years at a plate convergence rate of 30 mm/yr leaves a huge seismic deficit. Stress modeling results in a thrusting regime, consistent with the plate motion orientation along the Sagami trough, show that the Coulomb failure stress has increased on *Shishikura's* [2003] entire easternmost fault plane, theoretically bringing it closer to failure. However, *Ozawa et al.* [2003] discovered the signal of slow earthquakes on this part of the downgoing slab of the Philippine Sea plate that is located in the Sagami

trough southeast of the southern tip of Boso Peninsula. Two silent slip events with an interevent time of 6 years and slip of up to 20 cm were detected. If events like this happen on a regular basis, they can account for most or all of the accumulated plate motion predicted by the existing plate motion models [*Sella et al.*, 2002; *Seno et al.*, 1993, 1996; *Heki et al.*, 1999]. This would explain the very long recurrence intervals found for the Genroku-type earthquakes. These slow events may have slowly released stress buildup due to the 1923 evens in subsequent years, which could explain the very rapid cessation of the 1923 aftershock activity on central Boso Peninsula [*Hamada et al.*, 2001].

6.3. Deeper extension of Philippine Sea plate

According to *Ohtake* [1980] and *Bakun* [2004], based on earthquake and regional intensity data, respectively, the 1855 Ansei Edo earthquake ruptured the deeper extension of the Philippine Sea - northern Honshu plate interface (see also discussion in *Nyst et al.* [2005]). The 1923 earthquake increased the Coulomb stress on its own downward extension (Figure 6).

6.4. Western Sagami Bay Fracture

According to *Ishibashi* [1981, 1988] the Western Sagami Bay fracture (Figure 1A) is responsible for producing the Odawara earthquake, a periodic event with a repeat time of 73±4 year and average magnitude of M7.0 that also ruptured during the 1923 earthquake and even may have triggered it. The Western Sagami Bay fracture is a N-S trending fault in the Philippine Sea plate accommodating left-lateral strike-slip motion [*Nishimura and Sagiya,* 2004]. It probably developed to accommodate intraplate deformation between, in the west, the collision between the Izu-Bonin arc and Honshu and the associated cessation

of subduction and, in the east, ongoing subduction along the Sagami trough. The change in Coulomb failure stress on the Western Sagami Bay fracture due to the 1923 Kanto earthquake is positive (Figure 8) and may have triggered the 1930 $M_s = 7.3$ Kita-Izu earthquake [*Matsuda,* 1972] (Figure 8). *Ishibashi* [1988] predicted the next Odawara earthquake to take place in 1996±4, but it has not yet happened. A possible explanation could be that a premature release of energy in the 1930 earthquake caused the delay of the next Odawara earthquake.

References

Ando, M., A fault-origin model of the Great Kanto earthquake of 1923 as deduced from geodetic data, *Bulletin of the Earthquake Research Institute, 49*, 19–32, 1971.

Ando, M., Seismo-tectonics of the 1923 Kanto earthquake, *J. Phys. Earth, 22*, 263–277, 1974.

Bakun, W. H., Magnitude and location of historical earthquakes in Japan and implications for the 1855 Ansei Edo earthquake, *in preparation*, 2004.

Furumura, T., Seismic intensity distribution and source mode of the 1855 Ansei Edo earthquake: examination by numerical simulations (*in Japanese*), , , –, 2003. (ask Bill)

Hamada, N., K. Yoshikawa, M. Nishiwaka, M. Abe, and F. Kusano, A comprehensive Study of Aftershocks of the 1923 Kanto Earthquake, (*in Japanese*), *Zisin (Bull. Seis.*

Soc. Japan), *54,* 251–265, 2001.

Harris, R., Introduction to special section: Stress triggers, stress shadows, and implications for seismic hazard, *J. Geophys. Res., 95,* 24,347–24,358, 1998.

Heki, K., S. Miyazaki, H. Takahashi, M. Kasahara, F. Kimata, S. Miura, N. Vasilenko, A. Ivaschenko, and K.-D. An, The Amurian Plate motion and current plate kinematics in eastern Asia, *J. Geophys. Res., 104,* 29,147–29,155, 1999.

Huchon, P., and H. Kitazato, Collision of the Izu block with central Japan during the Quaternary and geological evolution of the Ashigara area, *Tectonophysics, 110,* 201–210, 1984.

Ishibashi, K., Specification of a soon-to-occur seismic faulting in the Tokai district, central Japan, based upon seismotectonics, in *Earthquake Prediction; an International Review,* edited by D. Simpson and P. Richard, pp. 297–332, AGU, Washington, D.C., 1981.

Ishibashi, K., "Kanagawaken-Seibu-Earthquake" and earthquake prediction I, (*in Japanese*), *Kagaku, 58*, 537–547, 1988.

Ishida, M., Geometry and relative motion of the Philippine Sea Plate and Pacific plate beneath the Kanto-Tokai district, Japan, *J. Geophys. Res., 97*, 489–513, 1992.

Ishida, M., and M. Kikuchi, A possible foreshock of a future large earthquake near Odawara, center Japan, *Geophys. Res. Lett., 19*, 1695–1698, 1992.

Jaeger, J. C., and N. G. W. Cook, Fundamentals of Rock Mechanics, 513 pp., Methuen, New York, 1969.

Kanamori, H., and S. Miyamura, Seismometrical re-evaluation of the Great Kanto earthquake of September 1, 1923, *Bull. Earthq. Res. Inst., 48*, 115–125, 1970.

Kanamori, H., Faulting of the Great Kanto earthquake of 1923 as revealed by seismological data, *Bull. Earthq. Res. Inst., 49*, 13–18, 1971.

Lin, J., and R. S. Stein, Stress triggering in thrust and subduction earthquakes and stress interaction between the southern San Andreas and nearby thrust and strike-slip faults, *J. Geophys. Res., 109*, B)2303, doi:10.1029/2003JB002607, 2004.

Matsuda, T., Surface faults associated with the Kita-Izu earthquake of 1930 in Izu Peninsula, Japan, in *The Izu Peninsula,* edited by M. Oshino and H. Aoki, pp. 77–93, Tokai Univ. Press, Tokyo, 1972.

Matsuda, T., Y. Ota, M. Ando, and N. Yonekura, Fault mechanism and recurrence time of major earthquakes in Southern Kanto district, Japan, as deduced from coastal terrace data, *Geol. Soc. Amer. Bull., 89,* 1610–1628, 1978.

Matsu'ura, M., T. Iwasaki, Y. Suzuki, and R. Sato, Statical and dynamical study on faulting mechanism of the 1923 Kanto earthquake, *J. Phys. Earth, 28*, 119–143, 1980.

Matsu'ura, M., and T. Iwasaki, Study on coseismic and postseismic crustal movements associated with the 1923 Kanto earthquake, *Tectonophys, 97*, 201–215, 1983.

Nishimura, T., and T. Sagiya, Crustal block kinematics around the northern Philippine Sea plate, central Japan, estimated from GPS and leveling data, , 2004.

Noguchi, S., Earthquake clusters in the Kanto and Tokai subduction zones: Implications for modes of plate consumption, in *Seismotectonics in Convergent Plate Boundary,* edited by Y. Fujinawa and A. Yoshida, pp. 451–467, TERRAPUB, Tokyo, 2002.

Nyst, M., T. Nishimura, F. F. Pollitz, and W. Thatcher, The 1923 Kanto earthquake re-evaluated using a newly augmented geodetic data set, *submitted to J. Geophys. Res.*, 2004.

Ohtake, M., A unified seismotectonic model for Kanto and Tokai regions: mechanics of shallow south Kanto earthquakes, *in Japanese, Bosai-Kagaku-Gijyutsu, (NIED report), 41,* 1–7, 1980.

Okada, Y., Surface deformation due to shear and tensile faults in a half space, *Bull. Seismol. Soc. Am., 75,* 1135–1154, 1985.

Okada, Y., Internal deformation due to shear and tensile faults in a half-space, *Bull. Seis. Soc. Am., 82,* 1018–1040, 1992.

Okada, Y., How soon until the next large south Kanto district earthquake?, *Earth Monthly, special issue 34,* 94–104, 2001.

Ozawa, S., S. Miyazaki, Y. Hatanaka, T. Imakiire, M. Kaidzu, M. Murakami, Characteristic silent earthquakes in the eastern part of the Boso peninsula, Central Japan S. Ozawa, *Geophys. Res. Lett., 30,* 1283, 10.1029/2002GL016665, 2003.

Pollitz, F. F., X. Le Pichon and S. J. Lallemant, Shear partitioning near the central Japan triple junction: the 1923 great Kanto earthquake revisited - II, *Geophys. J. Int., 126,* 882–892, 1996.

Reasenberg, P. A., and R. W. Simpson, Response of regional seismicity to the static stress change produced by the Loma Prieta earthquake, *Science, 255,* 1687–1690, 1992.

Sagiya, T., S. Myazaki and T. Tada, Continuous GPS array and present-day crustal deformation of Japan, *Pure Appl. Geophys., 157,* 2303–2322, 2000.

Sato, H., N. Hirata, K. Koketsu, D. Okaya., S. Abe, R. Kobayashi, M. Matsubara, T. Iwasaki, T. Ito, T. Ikawa, T. Kawanaka, K. Kasahara, S. Harder, Earthquake Source Fault Beneath Tokyo, *Science, 309,* 462–464 , 2005.

Sella, G. F., T. H. Dixon, and A. Mao, REVEL: A model for Recent plate velocities from space geodesy, *J. Gephys. Res., 107,* 10.1029/2000JB000033, 2002.

Seno, T., S. Stein, and A. E. Gripp, A model for the motion of the Philippine Sea plate consistent with NUVEL-1 and geological data, *J. Geophys. Res., 98,* 17941–17948, 1993.

Seno, T., T. Sakura, and S. Stein, Can the Okhotsk plate be discriminated form the North American plate? *J. Geophys. Res., 101,* 11,305–11,315, 1996.

Shishikura, M., Cycle of Interplate Earthquake Along the Sagam Trough, Deduced from Tectonic Geomorphology, *Bull. Earthq. Res. Inst. Univ. Tokyo, 78,* 245–254, 2003.

Shishikura, M., and S. Toda, *in preparation,* 2004.

Simpson, R. W., and P. Reasenberg, Earthquake-induced static stress changes on central California faults, in *The Loma Prieta, California Earthquake of October 17, 1989 - Tectonic Processes and Models,* edited by R. W. Simpson, *U. S. Geol. Surv. Prof. Pap.,* 1550-F, F55-F89, 1994.

Toda, S., R. S. Stein, P. A. Reasenberg, J. H. Dieterich, and A. Yoshida, Stress transferred by the 1995 $M_w = 6.9$ Kobe, Japan, shock: Effects on aftershocks and future earthquake probabilities, *J. Geophys. Res., 95,* 24,543–24,566, 1998.

Toda, S., and R. S. Stein, Response of the San Andreas Fault to the 1983 Coalinga-Nunez earthquakes: An application of interaction-based probabilities for Parkfield, *J. Geophys. Res., 107,* 10.1029/2001JB000172, 2002.

Tsukahara, H., and R. Ikeda, Hydraulic fracturing stress measurements and in-situ stress field in the Kanto-Tokai area, Japan, *Tectonophysics, 135,* 329–345, 1987.

Usami, T., Materials for comprehensive list of destructive earthquake in Japan, (*in Japanese*), *Univ. of Tokyo Press,* 1996.

Utsu, T., Seismicity of Japan from 1885 through 1925, it Bull. E.R.I, 54, 253–308, 1979.

Utsu, T., Seismicity of Japan from 1885 through 1925 (Correction and supplement), *Bull. E.R.I, 57,* 111–117, 1982.
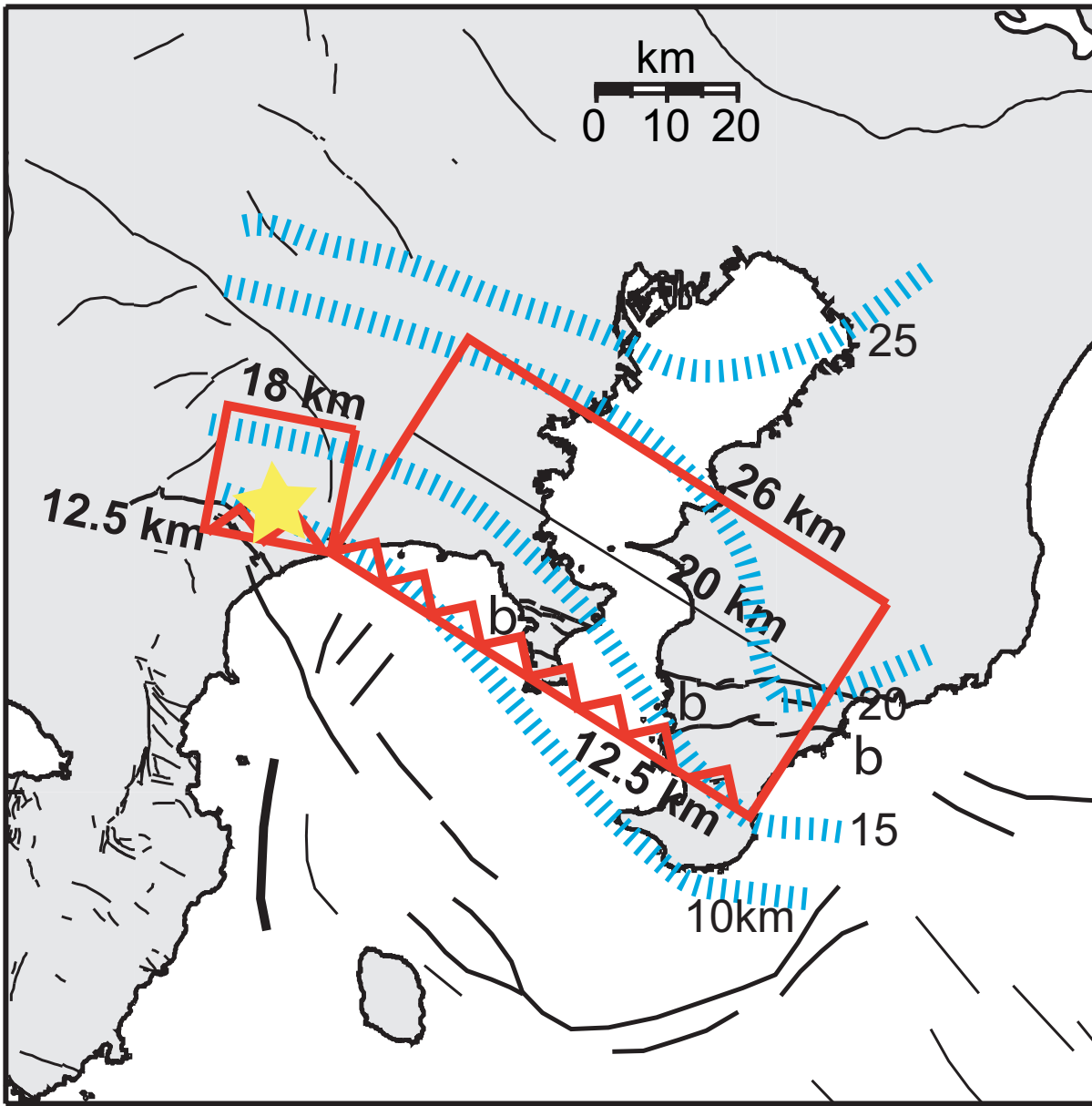
Wald, D. J., and P. G. Somerville, Variable-slip rupture model of the great 1923 Kanto, Japan, earthquake: Geodetic and body-waveform analysis, *Bull. seismol. Soc. Am., 85,* 159–177, 1995.

Wessel, P., and W. H. F. Smith, New, improved version of the Generic Mapping Tools Released, *EOS Trans. AGU, 79,,* 579, 1998.
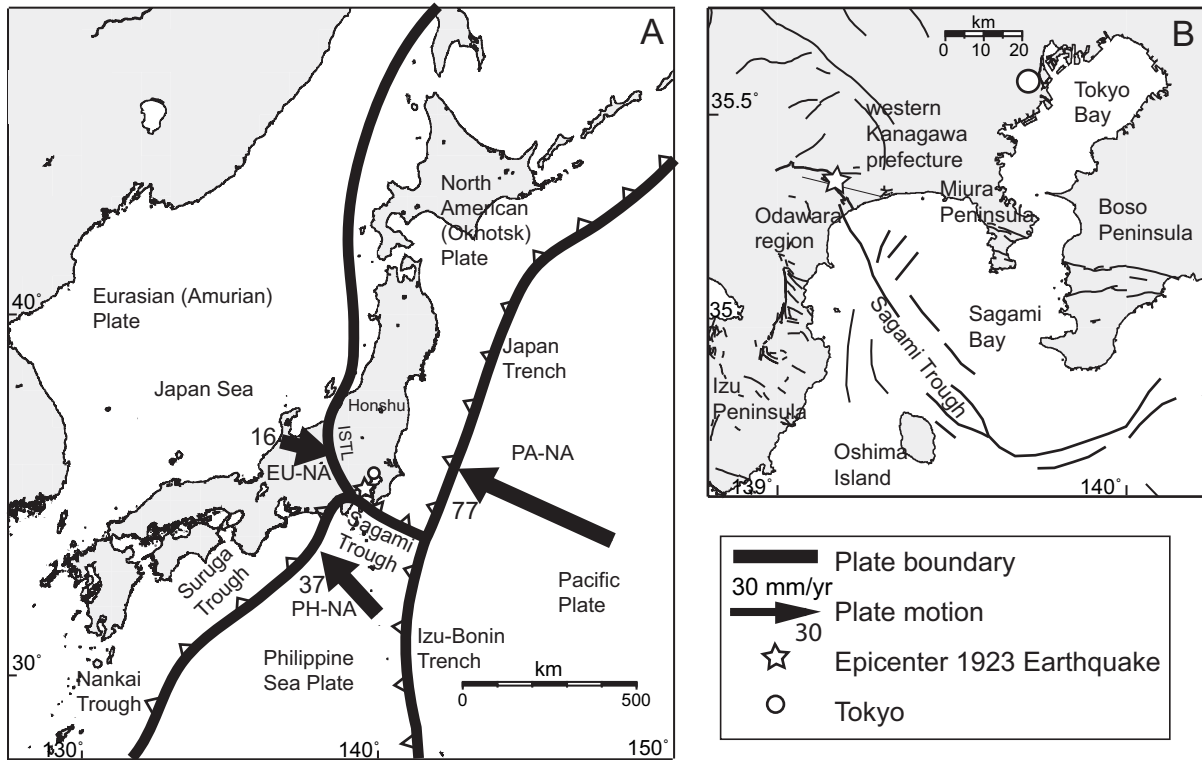
Figure 1. (A) Plate tectonic setting of Japan, where 4 major plates converge: the Eurasian (EU) or Amurian [*Heki et al.,* 1999; *Miyazaki and Heki,* 2001; *Sella et al.* 2002], North American (NA) or Okhotsk [*Seno et al.,* 1993, 1996; *Sella et al.,* 2002], Pacific (PA) and Philippine Sea (PH) plate. Northern Honshu is located on the North American or Okhotsk plate. ISTL Itoigawa-Shizuoka Tectonic Line. The arrows indicate motion relative to northern Honshu, the numbers are average rate predictions in mm/yr, based on Global Positioning System observations [*Heki et al.* 1999, *Seno et al.* 1996]. (B) Tokyo Bay and Sagami Bay.

Figure 2. (A), (B), and (C), modified from *Okada* [2001]: Changes in the seismicity distribution with time after the 1923 Kanto earthquake with respect to the period between 1884 and 1923. Shown are all events with magnitude ≥ 6 and depth ≤ 60 km. (A) Pre-earthquake seismicity from the historic earthquake catalogue of *Utsu* [1979, 1982]; (B) The first 10 years after the 1923 earthquake. Light-blue rings symbolize aftershocks from the catalogue of *Hamada et al.* [2001]. We have no records for the time interval 1924-1925. (C) Between 10 and 70 years after the 1923 earthquake. Earthquakes after 1925 come are the Japan Meteorological Agency (JMA) catalogue. (D) The first 4 months of aftershock activity following the 1923 Kanto earthquake from the catalogue of *Hamada et al.* [2001]. The catalogue contains the locations of about 400 earthquakes of which we show only those with accurate S-P times. Horizontal and vertical uncertainty in the location of aftershocks may be of the order of 20 km. The uncertainty in the locations of the off-shore aftershocks in the Sagami Bay is larger. Also shown are the two planes of the 1923 Kanto fault source model of *Nyst et al.* [2005]. Red dashes and numbers refer to the zones where changes in the seismicity pattern were detected after 1923: increased activity in (1) western Kanagawa Prefecture and on (2) Boso Peninsula, and decreased activity in (3) Tokyo and surroundings.

Figure 3. Active fault map of the coastal region around Sagami Bay with 1923 coseismic fault model planes of *Nyst et al.* [2005] and isodepth contours of the Philippine Sea plate [*Sato et al.*, 2005]. The star indicates the epicenter of the 1923 Kanto earthquake according to the seismic study of *Kanamori and Miyamura* [1970]. Bold printed lines indicate the Sagami Trough.
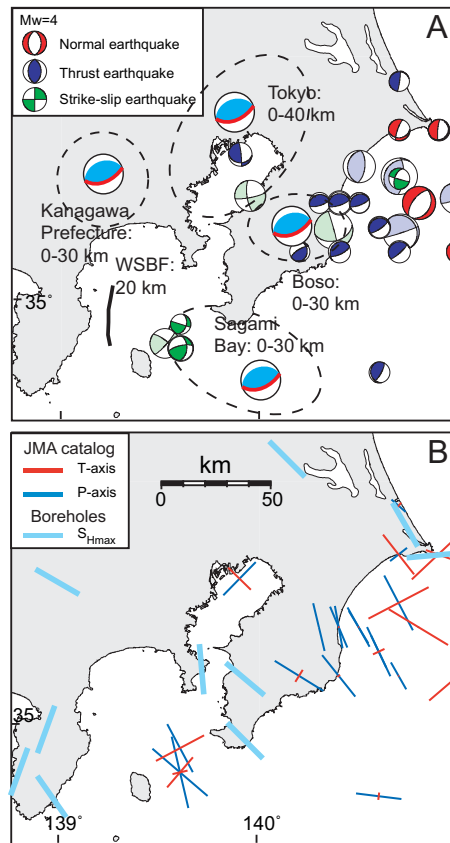
Figure 4. (A) and (B) Indicators of the regional stress field in Kanto: (A) Focal mechanisms with depths < 30 km and magnitude > 4. Solutions from the JMA catalogue are for the time interval 1997-2003, bold lines indicate solutions from the Harvard Centroid Moment Tensor (HCMT) catalogue between 1977 and 2003. The light blue beach balls indicate the preferred orientations of failure planes and they are shown in the areas where changes in seismicity pattern were detected after 1923 (see also Figure 2D) that are identified as source of seismic hazard. The preferred orientations of failure represent a local average of focal mechanisms of shallow earthquakes (M>2, depth ≤ 30 km) from the JMA catalogue that covers the time period from 1997 to 2003. WSBF Western Sagami Bay Fracture. (B) P- and T-axes of the earthquakes from the JMA catalogue (depths < 30km, time interval 1997-2003) and average orientations for the maximum horizontal stress component derived from hydraulic fracturing experiments in bore holes, ranging in depth from 100 to 800 m [*Tsukahara and Ikeda,* 1987].
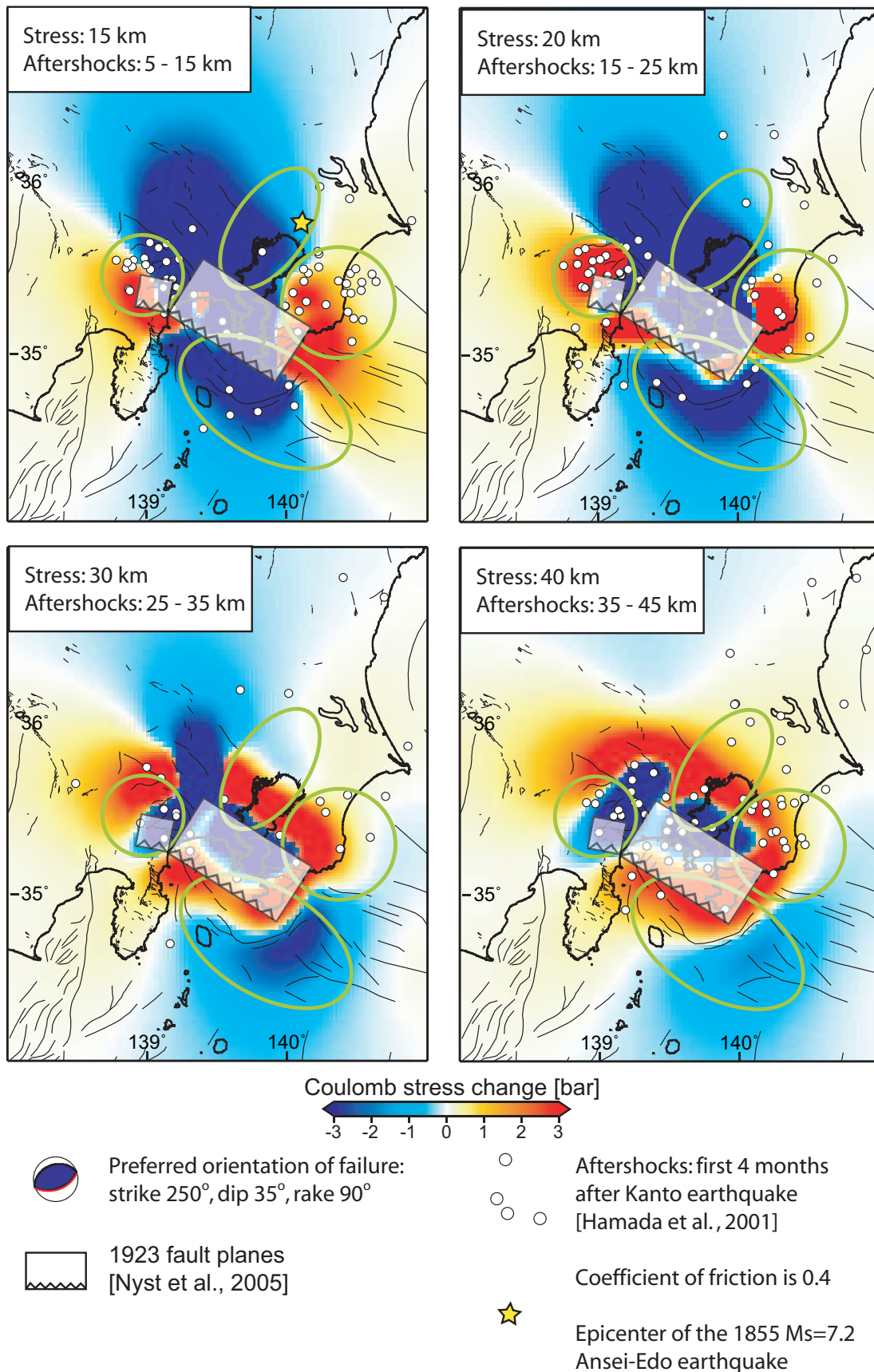
Figure 5. Change in Coulomb failure stress in the Tokyo Bay area computed with our 2-plane source model for the regional preferred orientation of failure (strike 250°, dip 35° and rake 90°) at different depth levels. The focal mechanism in the legend indicated the preferred orientation of failure with the red line representing the rupture plane. Seismicity shown is from the aftershock catalogue by Hamada et al. [2001] located between 0 and 40 km depth. The assumed coefficient of friction is 0.4.
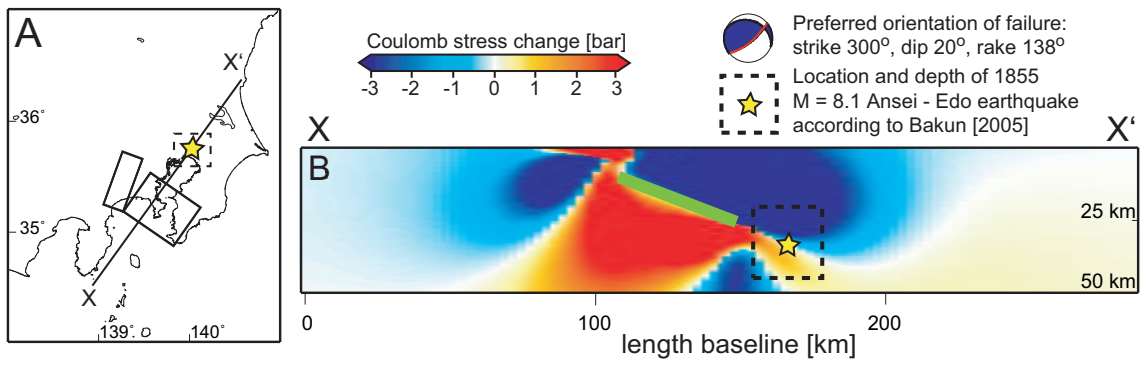
Figure 6. Cross-section of ΔCFS computed with our 2-plane source model on the extension of the 1923 Kanto fault plane (with the preferred orientation of failure taken from the large plane in our model: strike 300°, dip 20° and rake 138°). Seismicity shown is from the aftershock catalogue of *Hamada et al.* [2001] along the profile X-X'.

October 18, 2005, 4:01pm
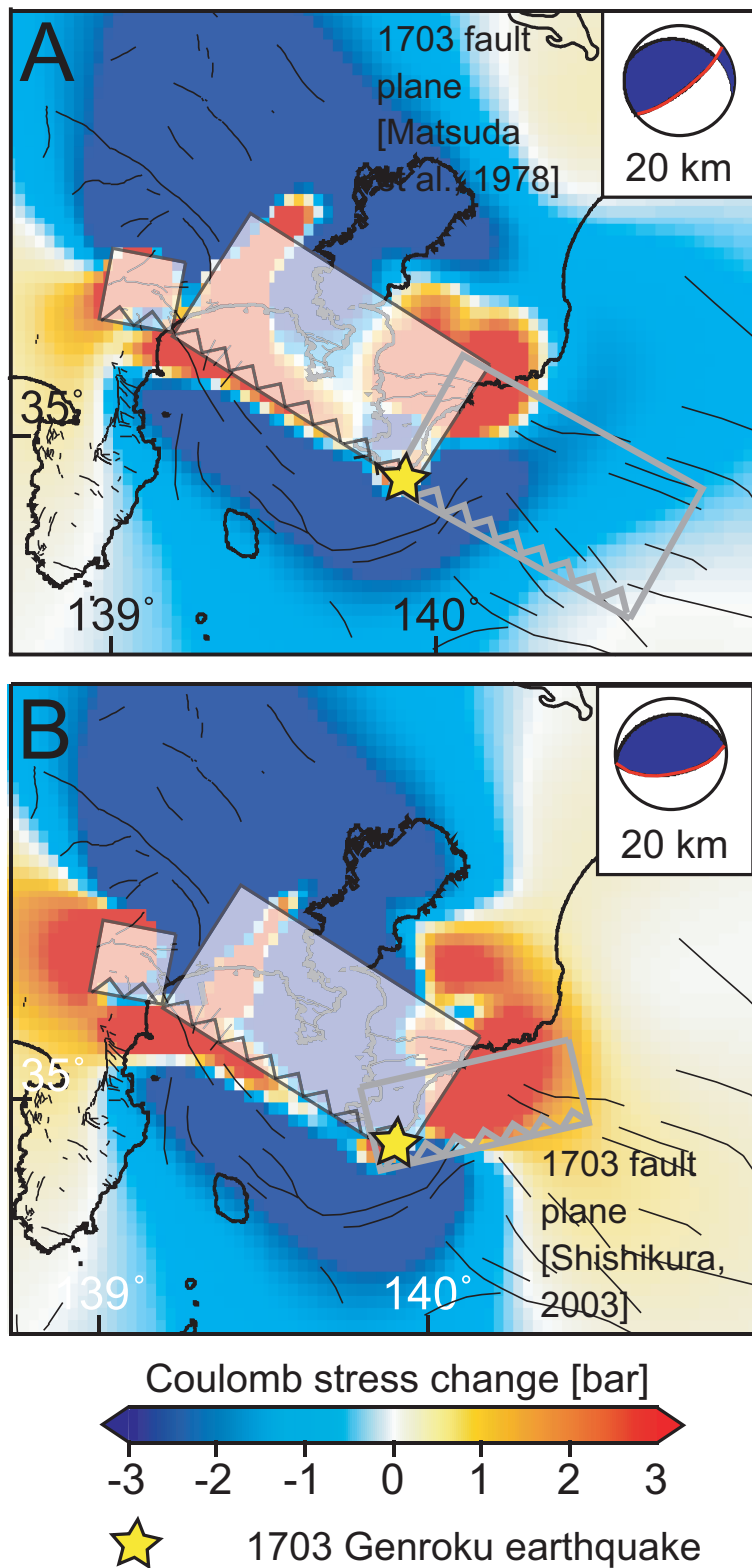
Figure 7. ΔCFS computed with our 2-plane source model for two different geometries of the easternmost fault plane of the 1703 Genroku earthquake. Seismicity shown is from the aftershock catalogue of *Hamada et al.* [2001] between 0 and 40 km depth. Stress field is computed at a depth of 30 km. (A) Fault plane after *Matsuda* [1978] with parameters taken from the large fault plane of our model: strike 290°, dip 27° and rake 145°; (B) Fault plane after *Shishikura* [2003] with strike 250°, dip 30° and rake 90°.
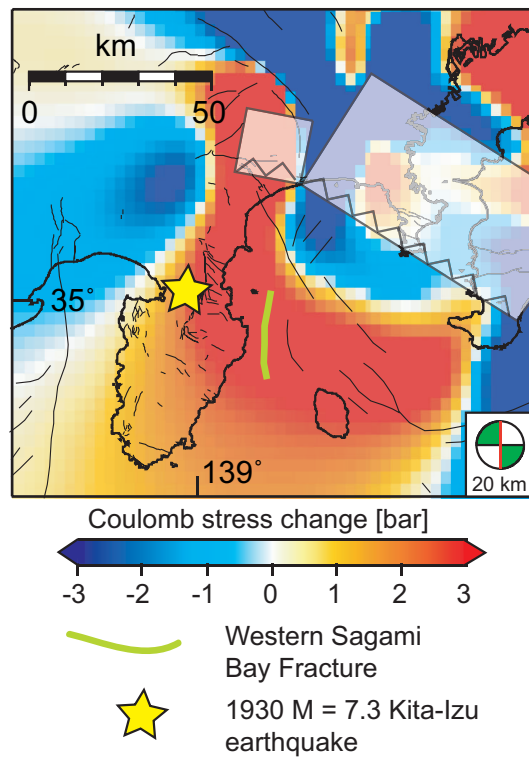
Figure 8. ΔCFS computed for the sinistral Western Sagami Bay Fracture (green line) at a depth of 20 km: strike 180°, dip 90° and rake 0°.